

A Large Magnetoresistance Effect in p–n Junction Devices by the Space-Charge Effect

Dezheng Yang,* Fangcong Wang, Yang Ren, Yalu Zuo, Yong Peng, Shiming Zhou, and Desheng Xue*

The finding of an extremely large magnetoresistance effect on silicon based p–n junction with vertical geometry over a wide range of temperatures and magnetic fields is reported. A 2500% magnetoresistance ratio of the Si p–n junction is observed at room temperature with a magnetic field of 5 T and the applied bias voltage of only 6 V, while a magnetoresistance ratio of 25 000% is achieved at 100 K. The current-voltage (*I*–*V*) behaviors under various external magnetic fields obey an exponential relationship, and the magnetoresistance effect is significantly enhanced by both contributions of the electric field inhomogeneity and carrier concentrations variation. Theoretical analysis using classical p–n junction transport equation is adapted to describe the *I*–*V* curves of the p–n junction at different magnetic fields and reveals that the large magnetoresistance effect originates from a change of space-charge region in the p–n junction induced by external magnetic field. The results indicate that the conventional p–n junction is proposed to be used as a multifunctional material based on the interplay between electronic and magnetic response, which is significant for future magneto-electronics in the semiconductor industry.

effect not only make the non-magnetic materials attractive to magnetic sensor industry, but also provide one of the most promising routes to realizing manipulation of the electron charge even spin in semiconductor devices by magnetic field.

Among these non-magnetic materials, silicon provides substantial benefits including the long spin coherence and the compatibility with the current CMOS technology, as well as the ability to fabricate low-cost devices. However, due to its modest carrier mobility it is experimentally and theoretically still a great challenge to obtain the large MR effect and related mechanism.^[6–15] One promising approach is based on the tunnel injection through the thin silicon dioxide layer, which triggers a transition to a high mobility transport regime by an autocatalytic process of impact ionization.^[6] At proper oxidation thicknesses (≈ 2 nm) the large MR ratios in lighted doped p-type silicon have been

1. Introduction

Magnetoresistance (MR) effects of non-magnetic materials such as silver chalcogenide,^[1,2] semimetallic bismuth,^[3] doped InSb,^[4] GaAs,^[5] and silicon^[6–15] have recently attracted a growing amount research interest due to their physical interests and potential applications in magneto-electronics devices. Compared with the magnetic materials, the MR effect on these non-magnetic materials presents two distinguished features. One is that the MR ratio is very large, comparable to, or even larger than, that of magnetic materials.^[16–19] The other is that the resistivity increases approximately linearly with the external magnetic field, even at mega-gauss fields. These features of MR

reported at 4 K and even at room temperature.^[6,7,15] An alternative way is to produce a quasi-neutrality breaking by applying a large electric field in silicon, in which the large MR effect is believed to arise from an electric-field inhomogeneity due to a space-charge effect.^[8,9] It is seen that these experiments provided implicit contributions for future silicon based magneto-electronics, however, the specific silicon substrates, millimeter-scale device size, and strict external conditions (e.g., oxidation layer thickness or large driven voltage 60 V) still hinder the further applications and developments in silicon-based magneto-electronics. Therefore a universal way to realize a large MR effect on silicon is still needed.

Although the theories^[23,24] and experiments^[13] have proposed that the electron and hole coexistence system can significantly enhance the MR effect due to the inverse carrier mobility between the electron and hole, there is still no definitive design to realize such coexistence system in experiments. The magnetodiode reported at the early stage can be considered a good coexistence system.^[25–28] By changing the electron and hole concentration under the magnetic field, a large MR effect is observed in the previous magnetodiodes. In these experiments, the carrier concentration becomes spatial variation, and then significantly changes the device resistance. However, these experiments only show that the MR effect in p–n junction can be caused by the carrier concentration gradient due to the artificial device geometries (e.g., different recombining surfaces

D. Z. Yang, F. C. Wang, Y. Ren, Y. L. Zuo,
Prof. Y. Peng, Prof. D. S. Xue
The Key Laboratory for Magnetism
and Magnetic materials of Ministry
of Education Lanzhou University
Lanzhou 730000, China
E-mail: xueds@lzu.edu.cn, yangdzh@lzu.edu.cn
Prof. S. M. Zhou
The Department of Physics
Tongji University
Shanghai 200092, China



DOI:10. 1002/adfm.201202695

or shape ratios), but do not show how the intrinsic space-charge region of p–n junction evolves or how the space-charge effect affects the MR effect in p–n junction.

In this work, we propose and realize an extremely large MR effect in convention silicon p–n junction devices by utilizing the external magnetic field to manipulate the space-charge region of the p–n junction. Our results show that the p–n junction device is robust, micrometer size scale, has a large MR ratio and high-field sensitivity, and operates over wide magnetic field and temperature ranges. Because the p–n junctions are fundamental elements and have been widely used in modern semiconductor industry, the magnetic field controlled p–n junction may represent a crucial step towards the future magneto-electronics in the semiconductor industry.

2. Results and Discussion

The structure of the device is Cu/Si(p+)/Si(n)/Si(n+)/Cu with a schematic representation shown in Figure 1a. At room temperature the carrier densities of Si(p+) and Si(n+) were $2.0 \times 10^{14} \text{ cm}^{-3}$ and $1.0 \times 10^{15} \text{ cm}^{-3}$, respectively. The device size of p–n junction was designed as $150 \mu\text{m}$, which is much smaller than the several millimeters in previous silicon devices.^[8–13] In contrast to the magnetodiode with lateral geometry, the structure Si(p+)/Si(n)/Si(n+) with vertical geometry is chosen to form a wide space-charge region. Without the limitation of recombining surface or shape ratio, the p–n junction with the vertical geometry can be more easily integrated into the modern semiconductor electronics with a much smaller device size. At the zero-magnetic field, the space-charge region between p-type and n-type silicon is uniform (Figure 1b). Its width depends on the equilibrium between the diffusion process and the built-in electric field. However, when the external magnetic field is applied, the equilibrium is broken. The carriers in n-type and p-type region are deflected by Lorentz force and accumulate at the edges of the sample (Figure 1c). As a result, a trapezoidal distribution in space-charge region is formed to balance the magnetic field. Because the transport properties of the p–n junction strongly depend on the configuration of space-charge region, the spatial distribution in space-charge region under the external magnetic field can drastically change the junction resistance.

To confirm such scenario for MR effect of p–n junction, the current-voltage (I – V) characteristics of p–n junction device were measured for various magnetic fields (H) with temperatures from 50 to 300 K. During the measurement the magnetic field was perpendicular to the current through the p–n junction.

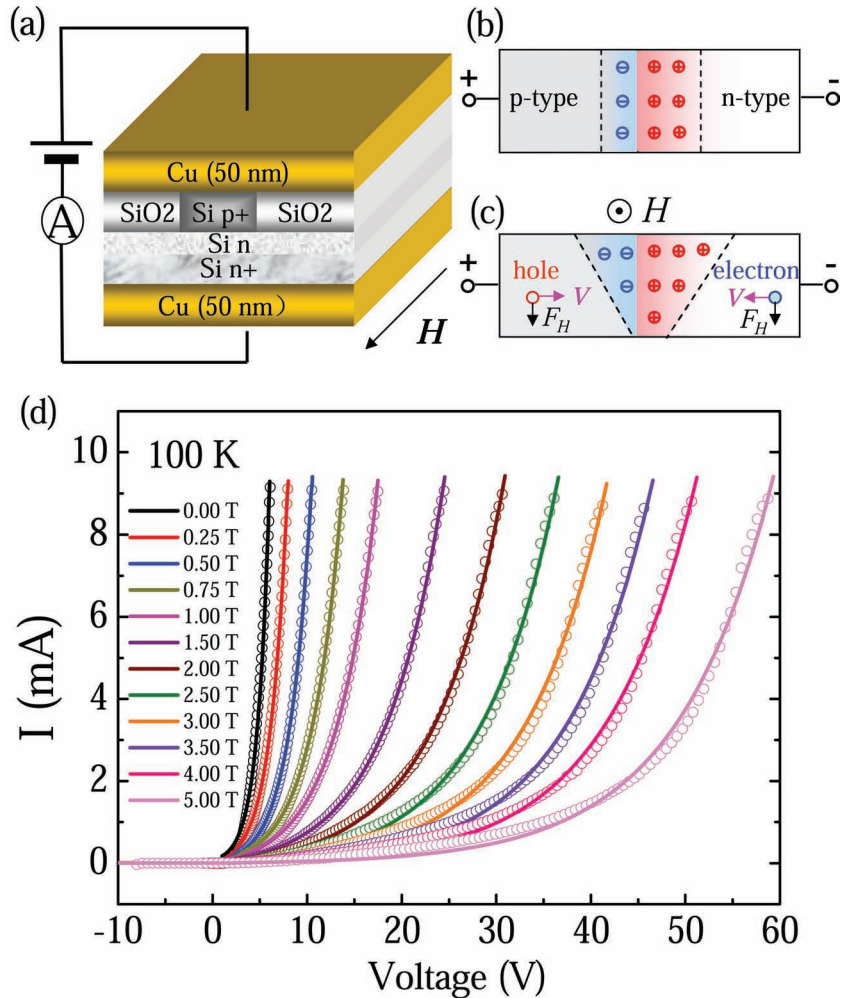


Figure 1. a) Schematic illustration of the p–n junction device structure and measurement sketch. The junction size is $150 \mu\text{m}$, separated by the SiO_2 layer. b,c) Schematic illustration of the origin of large MR effect in p–n junction due to the spatial distribution of space-charge region induced by the magnetic field. Panels (b,c) show sketches of the space charge-region of the p–n junction without and with the magnetic field, respectively. d) I – V characteristics of the p–n junction device at $T = 100 \text{ K}$ for various magnetic fields. From left to right the magnetic field is increased from 0 T to 5 T. The corresponding I – V curves fit with the equation $I = I_s(e^{\alpha V} - 1)$ are shown by the solid lines. Data points are the hollow circles.

Figure 1d shows the typical I – V characteristics of p–n junction device at 100 K. All the I – V curves present the obvious rectifying effect due to the intrinsic space-charge region in the p–n junction. For the zero-magnetic field I – V curve, the junction current is about 9 mA at $V = 6 \text{ V}$. However, as the external magnetic field is applied, a pronounced current suppression effect occurs and gradually increases with the increasing magnetic field, accompanied by enhanced positive MR effect. When $H = 5 \text{ T}$, at the same voltage bias 6 V the current is shifted downward to 0.03 mA, thus the corresponding MR ratio is more than 25000%. Here the MR ratio is defined as

$$\text{MR}(\%) = [R(H) - R(0)]/R(0) \times 100\%, \quad (1)$$

where $R(0)$ and $R(H)$ are the resistance (V/I) at zero and applied magnetic field, respectively. One can find that the I – V characteristics are more sensitive to the magnetic field in the larger

voltage bias regime, which demonstrates that an ultrathin barrier is an indispensable ingredient in creating the large magnitude of the MR effect.^[6]

Although the positive MR phenomenon was also observed in doped silicon,^[6–9] the transport behaviors and correlated mechanisms between doped silicon and p–n junction are distinctively different. For the doped silicon, the I – V characteristics typically obeyed the Ohm law at the low electric field and the Mott-Gurney law at high electric field.^[8,9] In contrast, for the p–n junction as shown in Figure 1d, the I – V curves under all magnetic fields are fitted well with the exponent equation

$$I = I_s(e^{\alpha V} - 1) \quad (2)$$

which is similar with the Shockley equation in the idealized p–n junction. Here α relates to the spatial distribution of the space-charge region and I_s represents the reverse saturation current. The exponential relationship of the p–n junction demonstrates that the transport properties of the p–n junction under magnetic field are still governed by the space-charge region in the p–n junction. Due to the different mechanisms between doped silicon and p–n junction, we notice that in order to observe appreciable MR ratio in the doped Si substrates, a large voltage bias of 60 V or appropriate current should be provided.^[8,9,13] However, here owing to the intrinsic space-charge region in the p–n junction, only a small voltage bias (≈ 6 V) is need to supply, independent of the strict external conditions.

In addition, we also note that the I – V characteristics under the magnetic field in our p–n junction device is different from those in the previous magnetodiode even if they have a similar p+–n–n+ junction structure. In the reported magnetodiode device the change of the I – V characteristics is dependent on the polarity of magnetic field.^[27] The junction resistance is increased (decreased) due to the low (high) carrier concentration when the carrier is deflected toward the high (low) recombining surface. For fixed driven voltage 6 V and magnetic 2 T, the MR ratio in our device is 400% at room temperature, while 30–100% MR ratio is observed in magnetodiodes.^[25,28]

The fitted parameters α and I_s as a function of the magnetic field with temperatures from 50 to 275 K are shown in Figure 2a,b, respectively. The values of α and I_s as a function of the magnetic field present significantly different behaviors. For all temperatures the α shows a monotonic decrease as the amplitude of magnetic field increases. At the zero magnetic field the value of α is the largest ($\alpha = 0.8$) and gradually decays to approach a constant value ($\alpha = 0.1$), whereas, I_s shows the non-monotonic behavior for all temperatures. It initially increases with increasing magnetic field to the maximum, and then decreases as the magnetic field further increases. The amplitude and position of the maximum I_s strongly depend on the temperature. As the temperature increases from 50 K to 275 K, the amplitude of the maximum I_s increases from 0.5 mA to 1.3 mA, and corresponding position also increases from 0.4 T to 4 T. Remarkably, as I_s gets to the maximum, the α approaches a constant value at the same time.

A natural explanation of our data is provided by the idea put forward in ref. [13], which considered the presence of the spatial distribution in space-charge region under the external magnetic field. Such distribution in space-charge region can

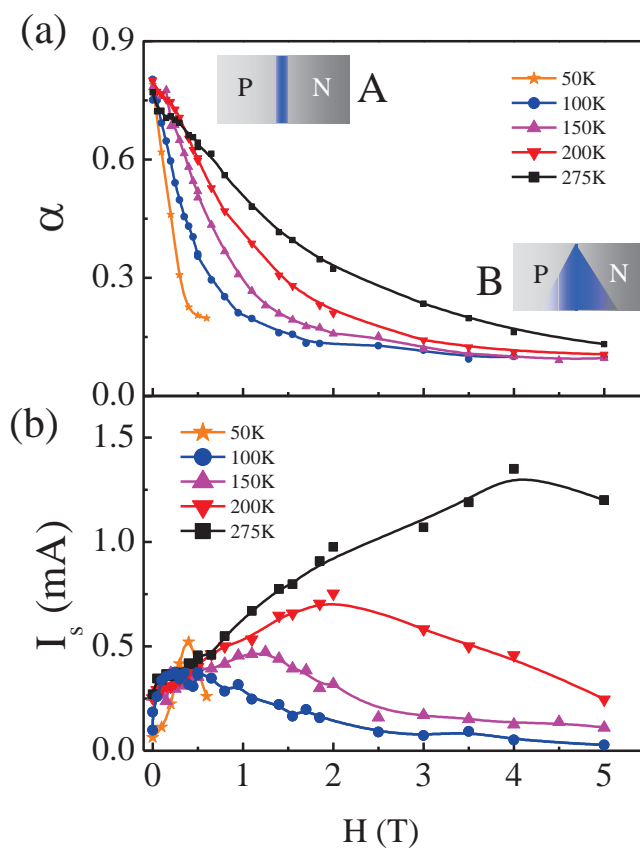


Figure 2. a,b) The magnetic field dependence of the fitted parameters α and I_s at various temperatures, respectively, by fitting the I – V curves with the equation $I = I_s(e^{\alpha V} - 1)$. The insets A and B in (a) demonstrate the possible stable distributions of the space-charge region at zero and large magnetic field.

introduce two important contributions of the MR effect. First, the spatial distribution of the space-charge region makes electric field inhomogeneous. As a result, carriers no longer move perpendicularly to the boundary. In this regime the current deflection significantly enhances the intrinsic transverse MR due to the residual Hall effect. This is also consistent with the previous reports in other nonmagnetic semiconductors, in which the spatial fluctuations in the conductivity were caused by the random distribution of doped impurities.^[20–24] Second, the spatial distribution of space-charge region changes the carrier concentrations. The carrier concentrations on each side of the p–n junction vary spatially with the applied magnetic field because of barrier spatial variations in the diffusion of carriers across the junction.

Therefore, according to the above discussions, the non-monotonic behavior of I_s as a function of magnetic field can be understood as a direct evidence by the competition between the carrier concentrations variation and the carrier scattering due to the electric-field inhomogeneity. When the external magnetic field is applied, the configuration of space-charge region becomes spatial distribution (shown in Figure 1c), making I_s enhancement due to a decrease of the barrier height between p and n region. However, as the magnetic field further increases,

the carrier scattering in inhomogeneous space-charge region becomes dominant, thus reduces the I_s . In contrast, the value of α from zero to high magnetic field is linked to the space-charge region configuration. The constant values of α at zero and high magnetic field ($H = 5$ T) might relate to the two stable space-charge region configurations, as shown the insets A and B in Figure 2a, respectively. However, we find that the values of α at zero and high magnetic field are independent of temperatures. This is still unclear and needs to be further studied. Finally, the temperature dependence of α and I_s as a function of magnetic field can be explained by the thermal emission during carrier diffusion through the space-charge region.

To further explore the origin of the MR effect in p–n junction device, we measured the p–n junction resistance and the MR curves as a function of temperature at constant current 10 mA. Although the MR ratio measured at constant current is much smaller than that at the constant voltage, the junction resistance at constant current can accurately represent the influence of the variation of space-charge region on the MR effect. As shown in Figure 3a, the temperature dependence of resistance is strongly affected by the amplitude of the magnetic field. At zero-magnetic field the resistance changes weakly with varying the temperature. In sharp contrast, for the intermediate magnetic field, such as from 0.3 to 1 T, as the temperature decreases, the

resistance starts to increase and then becomes more sharply at the lower temperature. We ascribe it as the both contributions of MR effect between the carrier concentration variations and the carrier scattering in inhomogeneous space-charge region. For the large magnetic field, such as from 2 to 5 T, in which the carrier scattering in inhomogeneous space-charge region plays a dominant role, the resistance almost linearly increases with decreasing temperature in the entire temperature regime.

The corresponding MR curves of p–n junction device in a temperature regime from 50 K to 300 K are presented in Figure 3b. Again, the MR ratio of the p–n junction increases with the H increasing, and the field sensitivity correspondingly increases with the temperature decreasing. For MR = 100% the magnetic field is 3 T and 0.3 T for $T = 300$ K and 50 K, respectively. one can find that the MR curves have a transition from parabolic to linear field dependence with decreasing temperature, demonstrating the inhomogeneous MR gradually plays a dominant role as temperature decreases, which is similar with the reported results in the doped silicon.^[8,9,13]

Obviously, the temperature dependence of MR is also strongly related with the temperature characteristics of the carrier concentration and the mobility in silicon. When the temperature increases from 50 K, the carrier concentration sharply increases due to the donor ionization. At about 100 K, most of donor atoms of silicon are ionized, thus the carrier concentration is virtually kept constant as the temperature further increases. In contrast with the carrier concentration, the carrier mobility significantly decreases when the temperature increases from 50 K to 300 K due to the lattice scattering.^[29]

Since the MR effect of p–n junction mainly stems from a change of space-charge region manipulated by the external magnetic field, as shown in Figure 1c, the carrier concentration and the carrier mobility play very important roles for the MR effect of p–n junction. When the magnetic field is applied, a carrier concentration gradient is formed due to the trapezoidal distribution of space-charge region. Such carrier concentration distribution strongly affects the junction resistance. It not only makes the electric field inhomogeneity, which deflects the current, but also directly determines the silicon resistivity itself. However, the carrier mobility contribution to the MR effect is closely linked to the Lorenz drift and the inhomogeneity scattering. As Lorenz drift increases due to an increase of the carrier mobility, the spatial distribution of the space-charge region is aggravated, thus the MR ratio and sensitivity are significantly enhanced. Furthermore, the increase of carrier mobility indicates that the inhomogeneity scattering is significantly enhanced, thus also enhance the MR effect. These can also explain the fact that the MR enhances with temperature decreasing, as shown in Figure 3b.

Finally, we calculated the I – V curves of a 2D idealized p–n junction under the external magnetic fields, by using the classical p–n junction equations.^[30]

$$q u_p p(x, y) \vec{E} - q D_p \nabla p(x, y) + q u_p p(x, y) (u_p \vec{E}) \times \vec{H} = 0 \quad (3)$$

$$q u_n n(x, y) \vec{E} + q D_n \nabla n(x, y) + q u_n p(x, y) (u_n \vec{E}) \times \vec{H} = 0 \quad (4)$$

$$\nabla \cdot \vec{E} = q(p(x, y) - n(x, y) + N_d - N_a)/\epsilon \quad (5)$$

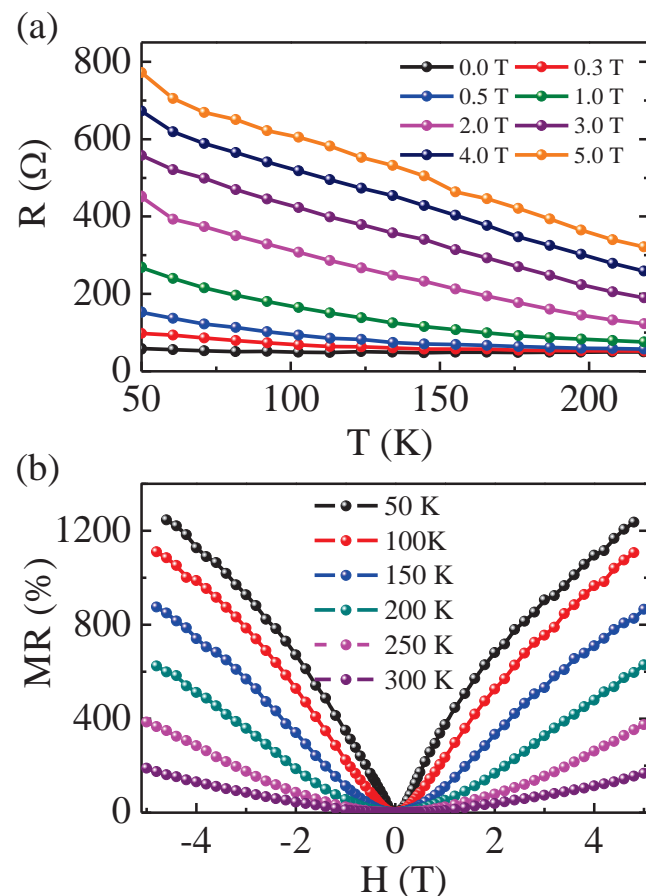


Figure 3. a) The temperature dependence of the resistance at $I = 10$ mA for different magnetic fields. b) The corresponding magnetoresistance curves for various temperatures.

Equation (3) and (4) represent the continuity equations of current in space-charge region for hole and electron, respectively. In these two equations, the total current includes the drift current (first term), the diffusion current (second term) and the current induced by Lorenz force (the third term). Equation (5) is the electrostatic equation (also known as Poisson equations), where the N_d and N_a are the uncompensated donors and acceptors in space-charge region, respectively. $p(x,y)$ and $n(x,y)$ are the hole and electron densities at position (x,y) , respectively. To simplify we assume that the boundary change of the space-charge region can balance the Lorenz force due to the concentration gradient and no generation-recombination current is formed inside the space-charge region. The whole p-n junction device is considered as a connection between the p and n region, in which the carrier mobilities for the hole and electron are taken $\mu_p = 0.048 \text{ m}^2 \text{ s}^{-1} \text{ V}^{-1}$ and $\mu_n = 0.135 \text{ m}^2 \text{ s}^{-1} \text{ V}^{-1}$ at room temperature, respectively. The calculated I - V curves for different magnetic fields are shown in Figure 4a. The simulated I - V curves of p-n junction can significantly be tuned by the magnetic field, particularly at the low magnetic field. This

suggests the carrier concentrations variation is more sensitive at the low magnetic field. More interestingly, we find the simulated I - V curves under magnetic fields still obey the Equation (1), demonstrating a manipulation of space-charge region by the external magnetic field. The fitted parameters α and I_s as a function of magnetic field are shown in Figure 4b. As the magnetic field increases, the α gradually decreases and I_s correspondingly increases due to the change of the space-charge region. It is seen that the simulated I - V behaviors show the same trend with our experimental data, although the simulated MR ratio is one order of amplitude smaller than that of experiment data. This deviation is believed to come from a lack of consideration of inhomogeneous scattering factor in the theoretical model. Moreover, because the simulation is independence of silicon structure itself, it indicates the MR effect based on p-n junction should be observed not only in silicon, but also in other semiconductors.

3. Conclusions

In summary, extremely large MR effects on conventional p-n junction based on silicon have been found. The MR ratio of the p-n junction is measured to be more than 2500% at room temperature and increases to over 25 000% at 100 K with a 5T external magnetic field and only 6 V bias voltage. The I - V curves under a wide range of temperatures and magnetic fields can be well fitted with an exponential relation. Electric-field inhomogeneity and carrier concentrations variation are found to directly affect the amplitudes of the MR effects in p-n junction. At the large magnetic field, the electric-field inhomogeneity plays an important role, while the carrier concentration variation is dominated at the low magnetic field. The theoretical analysis based on idealized two-dimension p-n junction shows a similar trend with the experimental data, which further reveals that the large MR effect stems from a change of the space-charge region induced by the magnetic field. Because our devices are identical to those used for conventional silicon diodes, the observation of large MR effect in p-n junction may indicate the conventional p-n junction possible to be a multifunctional device based on the interplay between electronics and magnetic response, which could open a new avenue for magneto-electronics.

4. Experimental Section

p-n Junction Device Fabrication: The samples were fabricated by the MEMS (micro electro mechanical systems). The wafers were light doped with $10^{12} \text{ atom/cm}^3$ n-type dopant in which surface resistivity was higher than $2000 \Omega \text{ cm}$. First, the wafers were cleaned with a routine RCA cleaning procedure. Then an oxidation film with a thickness of 6000 \AA was grown on the wafers in the oxidation furnace at $1030 \text{ }^\circ\text{C}$ for 4 h. After that, the patterns were transferred to the wafers by a lithography machine. The wafers were further treated with a boron implantation (40 keV , $2 \times 10^{14} \text{ atom/cm}^3$) at top surface and a phosphorus implantation (60 keV , $1 \times 10^{15} \text{ atom/cm}^3$) at back surface by a medium-energy ion implanter. Finally the 50 nm Cu electrodes at the top and bottom were sputtered separately with the vacuum $3 \times 10^{-5} \text{ Pa}$.

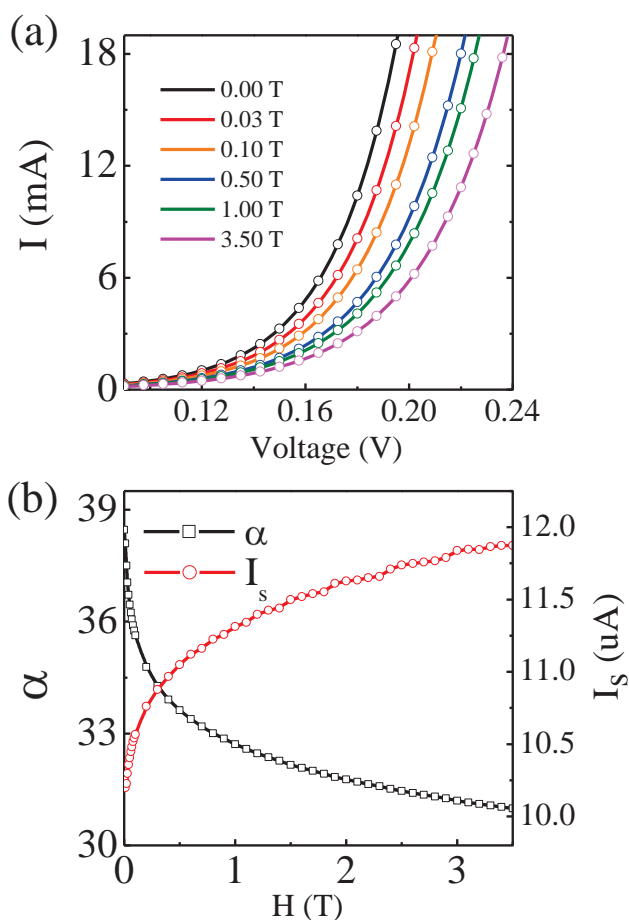


Figure 4. a) The calculated I - V characteristics of p-n junction at room temperature for various magnetic fields. The hollow circles refer to the fitting curves with equation $I = I_s(e^{\alpha V} - 1)$. b) The corresponding fitted parameters α and I_s as a function of external magnetic field.

Acknowledgements

This work is supported by National Basic Research Program of China (Grant No. 2012CB933101), the National Natural Science Foundation of China (Grand Nos. 50925103, 11034004, 11104122, 51201081).

Received: September 17, 2012

Revised: November 20, 2012

Published online: February 6, 2013

-
- [1] J. S. Hu, T. F. Rosenbaum, J. B. Betts, *Phys. Rev. Lett.* **2005**, *95*, 186603.
- [2] R. Xu, A. Husmann, T. F. Rosenbaum, M. L. Saboungi, J. E. Enderby, P. B. Littlewood, *Nature* **1997**, *390*, 57.
- [3] F. Y. Yang, K. Liu, K. M. Hong, D. H. Reich, P. C. Searson, C. L. Chien, *Science* **1999**, *284*, 1335.
- [4] S. A. Solin, T. Thio, D. R. Hines, J. J. Heremans, *Science* **2000**, *289*, 1530.
- [5] Z. G. Sun, M. Mizuguchi, T. Manago, H. Akinaga, *Appl. Phys. Lett.* **2004**, *85*, 5643.
- [6] J. J. H. M. Schoonus, F. L. Bloom, W. Wagemans, H. J. M. Swagten, B. Koopmans, *Phys. Rev. Lett.* **2008**, *100*, 127202.
- [7] J. J. H. M. Schoonus, J. T. Kohlhepp, H. J. M. Swagten, B. Koopmans, *J. Appl. Phys.* **2008**, *103*, 07F309.
- [8] M. P. Delmo, S. Kasai, K. Kobayashi, T. Ono, *Appl. Phys. Lett.* **2009**, *95*, 132106.
- [9] M. P. Delmo, S. Yamamoto, S. Kasai, T. Ono, K. Kobayashi, *Nature* **2009**, *457*, 1112.
- [10] H. J. Jang, I. Appelbaum, *Appl. Phys. Lett.* **2010**, *97*, 182108.
- [11] T. E. Park, B. C. Min, I. Kim, J. E. Yang, M. H. Jo, J. Chang, H. J. Choi, *Nano Lett.* **2011**, *11*, 4730.
- [12] N. A. Porter, C. H. Marrows, *J. Appl. Phys.* **2011**, *109*, 07c703.
- [13] C. Wan, X. Zhang, X. Gao, J. Wang, X. Tan, *Nature* **2011**, *477*, 304.
- [14] L. H. Wu, X. Zhang, J. Vanacken, N. Schildermans, C. H. Wan, V. V. Moshchalkov, *Appl. Phys. Lett.* **2011**, *98*, 112113.
- [15] J. J. H. M. Schoonus, P. P. J. Haazen, H. J. M. Swagten, B. Koopmans, *J. Phys. D: Appl. Phys.* **2009**, *42*, 185011.
- [16] S. A. Wolf, D. D. Awschalom, R. A. Buhrman, J. M. Daughton, S. von Molnar, M. L. Roukes, A. Y. Chtchelkanova, D. M. Treger, *Science* **2001**, *294*, 1488.
- [17] M. N. Baibich, J. M. Broto, A. Fert, F. N. Vandau, F. Petroff, P. Eitenne, G. Creuzet, A. Friederich, J. Chazelas, *Phys. Rev. Lett.* **1988**, *61*, 2472.
- [18] S. S. P. Parkin, C. Kaiser, A. Panchula, P. M. Rice, B. Hughes, M. Samant, S. H. Yang, *Nat. Mater.* **2004**, *3*, 862.
- [19] S. Jin, T. H. Tiefel, M. McCormack, R. A. Fastnacht, R. Ramesh, L. H. Chen, *Science* **1994**, *264*, 413.
- [20] V. Guttal, D. Stroud, *Phys. Rev. B.* **2005**, *71*, 201304.
- [21] J. Hu, M. M. Parish, T. F. Rosenbaum, *Phys. Rev. B* **2007**, *75*, 214203.
- [22] R. Magier, D. J. Bergman, *Phys. Rev. B* **2006**, *74*, 094423.
- [23] M. M. Parish, P. B. Littlewood, *Phys. Rev. B* **2005**, *72*, 094417.
- [24] M. M. Parish, P. B. Littlewood, *Nature* **2003**, *426*, 162.
- [25] E. I. Karakushan, V. I. Stafeev, *Sov. Phys. Solid State* **1961**, *3*, 493.
- [26] H. Pfeleiderer, *Solid-State Electron* **1972**, *15*, 335.
- [27] G. A. Egiazaran, G. A. Mnatsakanyan, V. I. Murygin, V. I. Stafeev, *Sov. Phys. Semicond.* **1976**, *9*, 829.
- [28] A. Mohaghegh, S. Cristoloveanu, J. De Poncharra, *IEEE Trans. Electron Devices* **1981**, *28*, 237.
- [29] F. J. Morin, J. P. Maita, *Phys. Rev.* **1954**, *28*, 96.
- [30] B. G. Streetman, S. K. Banerjee, *Solid State Electronic Devices*, Prentice-Hall Inc., Upper Saddle River, NJ **2006**, Ch.5.
-